https://ntrs.nasa.gov/search.jsp?R=20180005238 2020-05-10T05:25:06+00:00Z

Aeropropulsive Design Optimization of a Turboelectric Boundary Layer Ingestion Propulsion System

Justin S. Gray *
NASA Glenn Research Center, Cleveland, OH, 44139

Gaetan K.W. Kenway†
Science and Technology Corporation, Moffet Field, CA, 94035

Charles A. Mader‡ and Joaquim R. R. A. Martins §
University of Michigan, Ann Arbor, MI, 48109

I. Introduction

Boundary layer ingestion (BLI) for aircraft applications was first proposed by Apollo Smith and Howard Roberts in a 1947 paper that studied the use of jet intakes embedded in the boundary layer as a means to maintain laminar flow and reduce aircraft drag[1]. Aircraft applications for BLI didn't catch on then, but the idea was studied under the term "wake ingestion" for marine applications in the 1960's[2–4]. In 1993 interest in BLI for aircraft applications was renewed when Leyroy Smith published novel work using a boundary layer analysis combined with basic propulsion modeling to show the potential for significant fuel burn reduction[5]. Smith identified the tightly coupled aero-propulsive nature of BLI as a key challenge in the analysis and design of the concept. Betz had previously shown that BLI propulsion systems could have a propulsive efficiency of greater than 1, which made it an ill defined measurement for BLI, so Smith developed a new power based metric to evaluate the performance of BLI propulsion systems called the power saving coefficient (PSC) defined as

$$PSC = \frac{\mathrm{Pwr}'_{\mathrm{shaft}} - \mathrm{Pwr}_{\mathrm{shaft}}}{\mathrm{Pwr}'_{\mathrm{shaft}}}. \tag{1}$$

Significant further work by Drela[6], noting the difficulty of traditional thrust/drag force accounting for BLI systems, proposed an unified power balance accounting scheme that allowed the calculation of the power saving coefficient in a consistent and well defined manner.

A number of conceptual design studies have examined the aircraft level benefits of BLI propulsion systems [7–12], considering a wide range of fuselage and propulsor configuration. The findings of these various papers demonstrated the potential for BLI to offer significant reductions in aircraft fuel burn, however these conclusions were based on uncoupled models of the BLI system. This paper focuses on NASA's STARC-ABL concept, which utilizes a BLI propulsion system with a mostly conventional tube-with-wings layout. The STARC-ABL propulsion system is a turboelectric design consisting of two under-wing turbofan engines with generators attached that send power to the an electric motor driving the aft-mounted BLI propulsor. Given the layout of the propulsion system, one of the central design questions is relative size of the two propulsor types to get the best aircraft level performance. Addressing this question requires quantifying the improvement in efficiency of the BLI propulsor vs the under wing engines.

In prior work, the authors have demonstrated the importance of using a fully coupled aeropropulsive model to predict BLI performance [13]. We have shown that the coupled model predicts a lower total pressure in the inlet and a different surface pressure distribution on the fuselage compared to an uncoupled model. We furthermore performed a design study focused on the question of relative propulsor sizing, via a series of aeropropulsive design optimizations of the BLI and podded propulsors. Our results showed that the BLI system offered between 1% and 4.5% reduction in total power required for cruise, depending on the assumption made about the power transmission efficiency (η_{trans}) of the turboelectric system.

*Aerospace Engineer PSA Branch, 21000 Brookpark Rd., MS 5-11; Doctoral Candidate Department of Aerospace Engineering, University of Michigan; AIAA Member
†Aerospace Engineer, Science and Technology Corporation; AIAA Senior Member
‡Research Investigator, Department of Aerospace Engineering, AIAA Senior Member
§Professor, Department of Aerospace Engineering; AIAA Associate Fellow

The design study further demonstrated the importance of using a fully coupled aeropropulsive model, and established η_{trans} as a key design assumption for the overall design and performance of the aircraft. However, the aerodynamic models were constructed from an simplified axisymetric fuselage and BLI propulsor. While these models were sufficient to establish the key trends, recent aerodynamic analysis of the configuration has clearly shown that 3 dimensional aerodynamic models are necessary in order to accurately predict the airflow at the aft fuselage.

Kenway an Kiris examined the inlet distortion for the BLI propulsor on the aft-fuselage of the STARC-ABL configuration, concluding that aerodynamic shape optimization was able to reduce distortion to less than 2%[14]. They performed optimizations of both the bare fuselage and a fuselage with wings attached (but without a vertical tail), finding that the wing downwash has a strong impact on the flow and created additional distortion not present in the fuselage only configuration. Beyond the conclusions about distortion, their results clearly demonstrate the importance of using 3 dimensional models of the airframe, including the wings, for the aerodynamic analysis. In that work nacelle design variables included only allowed for shape changes at the front section of the nacelle. Significant changes to the nacelle diameter, the shape of the nozzle plug, or to the shape at the aft of the nacelle were not part of the design space. The somewhat limited design freedom present was sufficient for the distortion minimization objective function they used, but is not sufficient to consider large variations in the propulsor sizing.

In this work we perform aeropropulsive design optimization of the BLI propulsor, at a cruise condition of Mach .785 and altitude of 37000 ft. The optimization is performed using SNOPT [15], a sequential quadratic programming algorithm gradient. The coupled model was constructed in the OpenMDAO framework[16] with a RANS CFD aerodynamic analysis coupled to a 1D thermodynamic cycle model of both the under wing and aft mounted propulsors. All analyses provide analytic derivatives, and OpenMDAO is used to compute the coupled derivatives across the aeropropulsive model.

The propulsor is designed minimize the shaft power required to generate a given net force on the entire aircraft (fuselage, wings, tail, propulsor). Distortion is computed using the method developed by Kenway and Ceris, but is not specifically constrained in the optimization. The optimization is run for a series of different propulsor sizes to study the impact of propulsor sizing on BLI performance.

II. Aerodynamic Model

A. RANS Solver: ADflow

The aerodynamic analysis is modeled using the ADflow code, running a RANS analysis using overset meshes generated using the Chimera Grid Tools and an implicit hole cutting scheme[17, 18]. The mesh, show in Figure 2, is composed of 8 different sub-meshes totaling 6 million cells in all.

The geometry shown in Figure 2 is modeled with the openVSP geometry engine[19], which outputs a surface

Fig. 1 Rendering of the STARC-ABL aircraft configuration

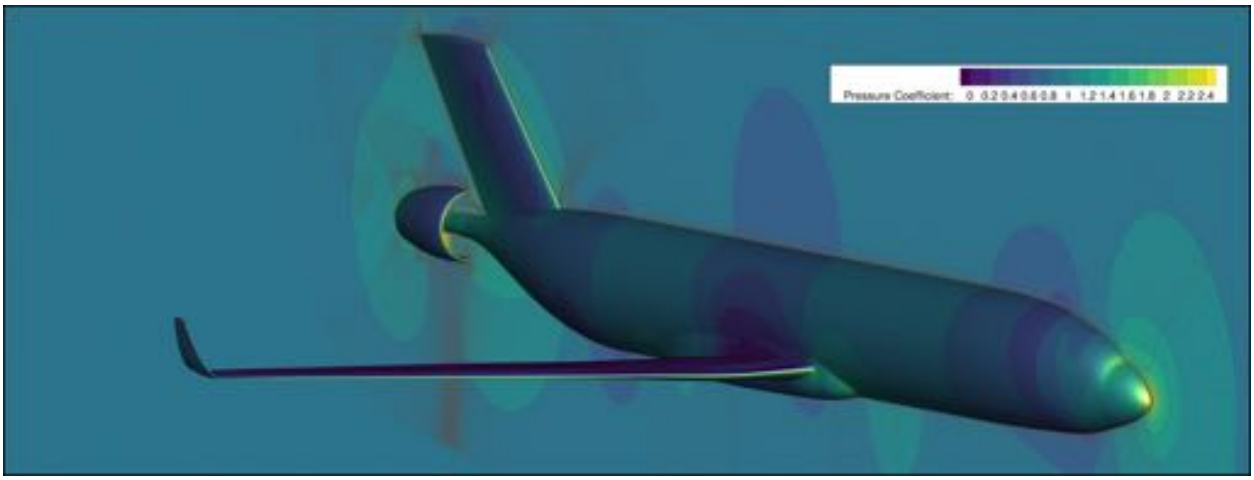

Fig. 2 Overset mesh of of the model with surface C_p color contours.

discretization for each body in the mesh individually. Then a rigid links interpolation scheme is used to connect the surface openVSP surface discretization to the surface discretization of the CFD mesh. Changes in the surface mesh are propagated to the volume mesh via an inverse distance weighting implementation of mesh-morphing following the formulation of Luke et al.[20]

The aircraft wing was optimized for minimum drag in prior work, using a 5 point multipoint stencil around the cruise condition. The wing geometry was held fixed at this previously optimized design for all studies done in this work. The BLI propulsor is modeled using a body-force zone[21] that imparts the effect of the fan on the flow without needing to model the fan itself.

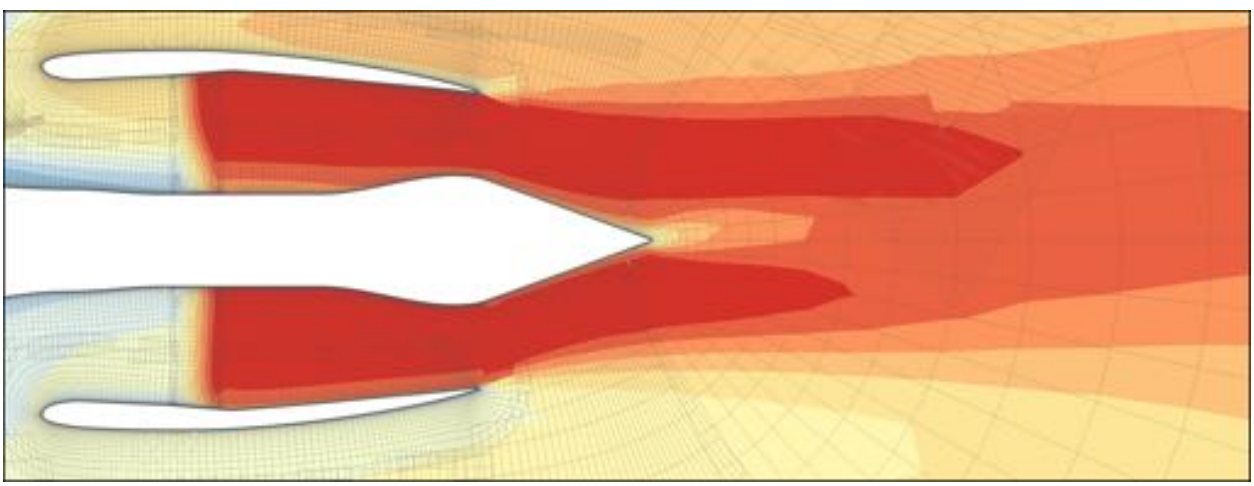

Fig. 3 Side view of the aft mounted BLI propulsor including the body force zone that simulates the fan. The p_t color contours show the effect of the van via the increased pressure.

B. Force Accounting

In order to provide a consistent force accounting scheme, all forces are computed by integrating pressure, viscous, and momentum-flux forces across all the boundary conditions in the model. Additionally, the body force zones that simulate the fans for the BLI and under wing propulsors contribute their respective additional thrusts. The total force coefficient on the aircraft is computed as follows:

$$C_F = \frac{2}{\rho_\infty V_\infty^2 A_{\text{ref}}} \left[\iint_S \left(\left((p - p_\infty)\hat{\boldsymbol{n}} + \vec{\boldsymbol{f}}_{\text{visc}} \right) \right) dS + (\vec{F}_{\text{BLI}} \cdot \boldsymbol{n}\hat{_{\text{BLI}}}) \right]. \tag{2}$$

In equation (2), F_{BLI} represents the force contribution from body-force zone of the aft propulsor. This is not the same as the net force from that propulsor, but rather is the net force that would be felt by the fan itself. The net force would need to be computed by combining $\vec{F}_{\text{BLI}}$ with the forces integrated over the surface of the propulsor, but this quantity is not explicitly computed in this work. C_F represents the net force coefficient of the entire wing-fuselage-tail-propulsor system, and as such it is a signed quantity. A positive value indicates a net decelerating on the body, while a negative value indicates a net accelerating force on the body. C_F does not include the contribution from the under-wing engines, which are modeled independently using a 1D propulsion model described in a later section of the paper. For a cruise condition with a constant velocity the net force coefficient of the entire aircraft should be 0, but C_F will have a positive quantity representing a net decelerating force. The remaining force necessary to achieve constant speed will be provided by the under-wing propulsors.

C. Computing BLI Propulsor Power

In order to interface with the propulsion model the power being used by the BLI fan needs to be computed via an volume integral over body force zone:

$$\text{Pwr}_{\text{flow}} = \iiint \left(\vec{V}_{\text{local}} \cdot \vec{\boldsymbol{f}}_{\text{local}} \right) dv, \tag{3}$$

where V_{local} is the local velocity vector and $\vec{\boldsymbol{f}}_{\text{local}}$ is the local body force contribution for the infinitesimal fluid volume.

Note that equation (3) computes only the power imparted to the flow by the fan, which does not equal the total shaft power needed to drive the fan. The shaft power and the flow power differ because of the fan adiabatic efficiency, η_{fan} This fan efficiency is accounted for in the propulsion model.

III. Propulsion Model

A. 1D Cycle Model: pyCycle

The propulsion model used is a 1D thermodynamic cycle model, built with pyCycle[22, 23]. pyCycle is a modular cycle modeling capability similar to the industry standard NPSS[24] but with the added feature of offering analytic derivatives for use in optimization applications. Propulsion models are build up from cycle elements such as *Compressor Turbine*, *Combustor*, *Nozzle*, etc.

The 1 dimensional propulsion model requires scalar flow quantities as inputs, but the aerodynamic analysis computes the flow quantities as a nonuniform distribution over a 2D plane. So at the interface between the aerodynamic analysis and the propulsion model the 2D data needs to be averaged into equivalent 1D values, but it is important for this process to be done in a conservative fashion so that the correct net force on the boundary is retained in both analyses.

There are a number of different approaches to this averaging, which conserve different different flow quantities. Livesey compared a number of different methods, from the perspective of computing scalar values from rake data measured in a experiment [25, 26], concluding that an entropy conserving approach was the the most useful in that context because that ensured that physically meaningful pressure loss coefficients would be computed when the averaged values were compared at multiple axial locations.

In this application, the interface plane represents a transition from one analysis to another and the principal concern is that the net force on the interface plane is the same between the two analyses. The forces are governed by the static pressure and momentum flux through the interface plane so these are the quantities we seek to conserve.

In the aerodynamic analysis the force normal to any plane is computed by

$$F_S = \iint_S \left[(p - p_\infty) + \rho(V - V_\infty)(\vec{V} \cdot \hat{\boldsymbol{n}}) \right] dS. \tag{4}$$

If you assume uniform values across the plane, so the flow can be represented by scalar values, (4) simplifies to

$$F_S = \left[(\bar{p_s} - p_\infty) A_S + \dot{m} \left(\bar{V} - V_\infty \right) \right] \hat{\boldsymbol{n}}. \tag{5}$$

Over any given plane the total mass flow rate and area can be computed via

$$\dot{m} = \iint_S \rho \vec{V} \cdot \hat{n} dS \tag{6}$$

$$area = \iint_S dS. \tag{7}$$

Equating (4) and (5), canceling out the p_∞ and V_∞ terms, and separating the pressure and velocity components yields

$$\bar{p_s} = \frac{1}{A_S} \iint_S p dS, \tag{8}$$

$$\bar{V} = \frac{1}{\dot{m}} \iint_S V \rho (\vec{V} \cdot \hat{\boldsymbol{n}}) dS \tag{9}$$

Equations (8) and (9) indicate that a force conserving averaging scheme will ensure that the inflow conditions to the propulsion model should be chosen such that the static pressure matches the area averaged static pressure and the flow velocity should match the mass averaged velocity on the interface plane.

B. BLI Propulsor Model

Although the thrust from the BLI propulsor is modeled as via a body-force actuator zone in the aerodynamics model, a propulsion model is still needed to compute the shaft power required to produce that thrust. The BLI propulsor model is composed of four cycle elements: *CFD Start*, *Ambient*, *Fan*, and *Performance*.

The *CFD Start* element implements an implicit solve for the force conserving flow averaging scheme described previously. The implicit variables p_t, T_t, MN are solver for such that the static conditions to match the computed $\bar{P_s}, \bar{V}, area$ for a given $\dot{m}$. The *Ambient* component used a 1976 standard atmosphere to compute the free stream flow properties. The *Fan* and *Performance* handle the actual thermodynamic calculations that compute a required shaft power from the $\dot{m}$ and pressure ratio computed by the aerodynamic analysis. Figure 4 shows the connections between the 4 cycle elements of this model.

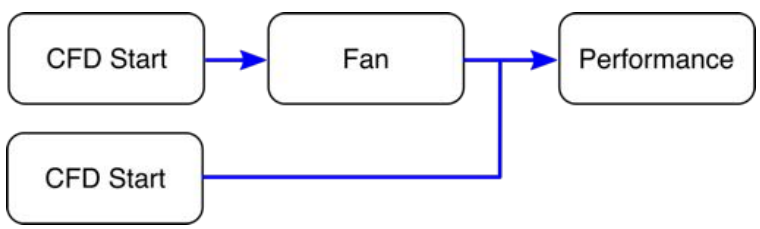

Fig. 4 Cycle elements in the pyCycle model of the BLI propulsor.

The fan efficiency is computed to such that polytropic efficiency, η_{poly} is held constant at 97%, which matches the technology assumptions for NASA's N+3 high bypass ratio turbofan engine [27]. The effect of holding a constant $\eta_{\text{poly}}$is that the adiabatic efficiency, $\eta_{\text{adiabatic}}$, of the fan — the quantity that directly impacts the shaft power— varies with respect to fan pressure ratio (FPR) and is always less than 97%. The resulting variation of $\eta_{\text{adiabatic}}$ with respect to FPR is shown Fig. 5. The trend is very nearly linear because of the very low FPR.

This model outputs the required generator power, which takes into account both the fan efficiency ($\eta_{\text{adiabatic}}$) and the power transmission efficiency (η_{trans}). The required generator power becomes an input to the under-wing engines, which includes it as an additional load on the lower pressure spool.

IV. Aero-Propulsive Optimization

A. Optimization Setup

The performance of the BLI system was analyzed at the cruise condition, Mach .785 and 37000 ft. For a steady cruise there will be zero net force over the entire aircraft, including the under-wing propulsors, wings, tail, fuselage and aft-propulsor. So a portion of the thrust will come from the under-wing propulsor and a portion from the aft-propulsor.

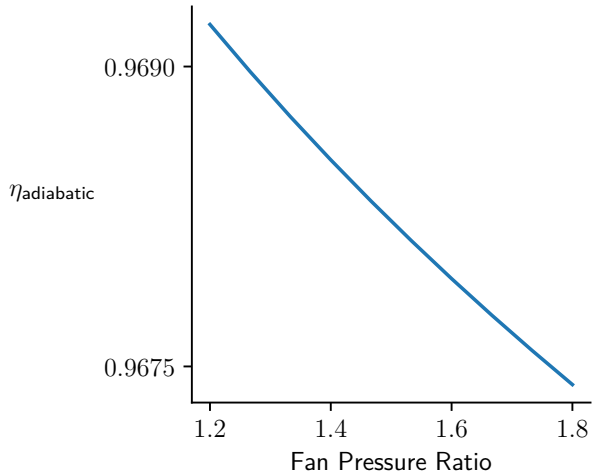

Fig. 5 Fan adiabatic efficiency vs FPR, assuming a constant polytropic efficiency of 97%

One primary consideration in the propulsion system design is what the correct split between the under-wing and aft propulsors should be to achieve the lowest overall fuel consumption. For a full aircraft design process addressing this question requires considering thermodynamic performance, propulsion system weight, aircraft center of gravity, etc. In this work we have modeled only the thermodynamic performance of the aft-propulsor, and hence can not fully address this design question. However, in recognition of the importance of propulsor sizing to the overall aircraft performance we consider optimized designs of BLI propulsors for three different sizes and compare their relative performance.

Each optimization was formulated to minimize the shaft power required by the BLI propulsor at the cruise condition with respect to fusleage shape design variables and propulsion design variables, subject to set of constraints. The full problem formulation is given in Table 1, which describes the 26 design variables and 14 constraints. Of those 14 the F_{net} constraint is the most physically significant because that is what ultimately sizes the BLI propupulsor. The 10 geometric thickness constraints are extremely cheap to evaluate because they do not involve the CFD analysis at all, so overall the problem requires just 4 expensive adjoints. The use of the nozzle pressure ratio constraint is notable here, because it is not normally a parameter used to govern the design of a fan. In this work, the NPR constraint was used in lieu of a constraint on FPR because it was found to be more numerically well posed for shape optimization of the propulsor duct.

Using a sign convention derived from the aerodynamic model with the origin located at the aircraft nose, positive values of net force represent a decelerative force on the body. Since the aerodynamic model only includes the aft propulsor, the F_{net} value computed from it represents the amount of net thrust required from the under-wing propulsors for a steady cruise condition. A larger F_{net} indicates larger under-wing propulsors and a smaller aft-propulsor.

Figure 6 shows the XDSM[28] of the optimization formulation, indicating how data is passed between the different analyses. The four different analyses are coupled using OpenMDAO, which both solves the nonlinear analysis and computes the total derivatives needed by the optimizer using an adjoint formulation.

In Figure 6, there is a component labeled *VSP Preprocessing*. The geometry engine for this work is OpenVSP, which is integrated directly inside the *ADflow* discipline. OpenVSP exposes a number of parameters that control the shape and diameters of cross-sections on both the fuselage, BLI nacelle and wing. However, for this work a number of those parameters were linked together, to provide a more physically meaningful geometry parameterization. For example, the sharp trailing edge of the nacelle is composed of two separate diameters: one for the upper surface and one for the lower surface. It is important that both these diameters are always forced to take the same value, so the geometry stays water tight. This is accomplished via the *VSP Preprocessing* component in the model which takes in a set of design variables and relates them to the actual openVSP model inputs.

The *ARP1420 Distortion* component implements the distortion metric from the "Gas Turbine Engine Inlet Flow Distortion Guidelines" ARP1420 standard[29], using the scheme developed by by Kenway and Keris [14]. The metric captures the magnitude of the variation in total pressure across the fan face both circumferentially and radially using data taken from multiple sensor locations distributed across the fan face. We use 5 radial measurement locations each with 30 sensors distributed evenly in the circumferential direction, yielding a total of 150 sensors. The five distortion

Table 1 Optimization problem definition for the aero-propulsive design of the propulsion system.

	Variable/Function	Description	Quantity
minimize	$\text{Pwr}_{\text{BLI-shaft}}$	Shaft power required for the BLI propulsor	
with respect to	F_{BLI}	BLI propulsor body-force applied	1
	X_{shape}	Shape variables for the fuselage and propulsor nacelle	25
		Total	26
subject to	$C_L = .5$	lift coefficient at cruise	1
	$g_{\text{geo}} = 0$	geometric thickness constraints	10
	$\text{NPR} > 1.65$	nozzle pressure ratio constraint	1
	$F_{\text{net}} = F^*_{\text{net}}$	required net force on the body	1
		Total	14

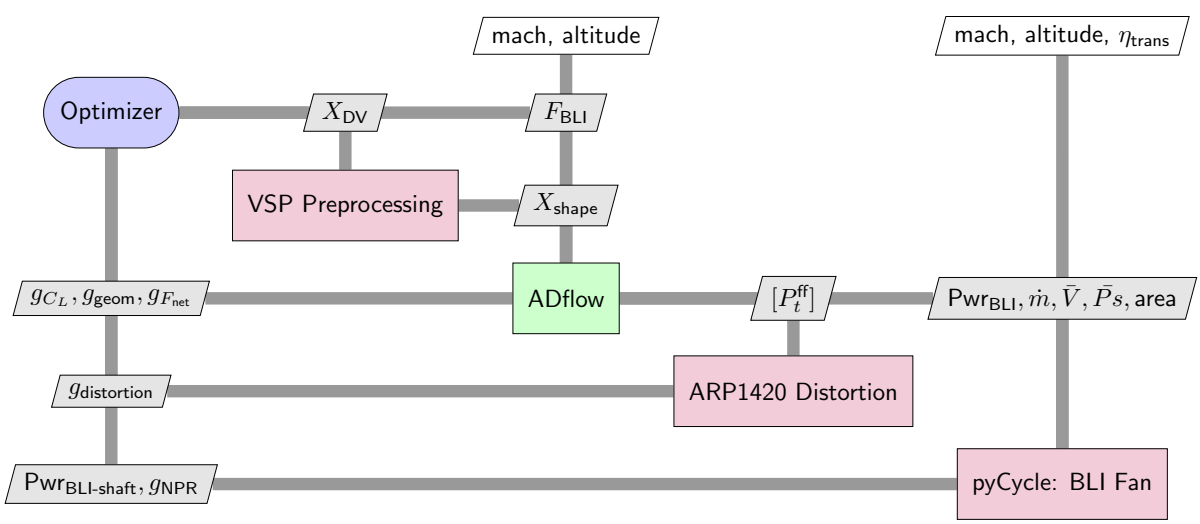

Fig. 6 XDSM diagram of the full optimization problem formulation.

measurements from each of the five radii are aggregated with a KS [30] function, giving a smoothed maximum value which can be used as a constraint on the optimization. In this work, the distortion was computed but not directly constrained.

B. Optimization Results

Three optimizations were performed for F^*_{net} values of 9000 N, 11000 N, and 13000 N. Key performance parameters from each optimization are reported in Table 2. The 9000 Newton case yields the largest aft-propulsor and hence requires the most shaft power. Compares to the 9000 Newton case, the 11000 Newtons case requires 22% more thrust from the under-wing propulsors and uses 14.6% less shaft power for the BLI propulsor. The 13000 Newton case requires 44% more thrust from the under-wing propulsors and uses 29.2% less shaft power for the aft propulsor. For all three cases, the constraint on NPR limits the fan pressure ratio from going below about 1.3.

The total pressure recovery, $p_t/p_{t\infty}$, and the distortion metric give somewhat inconclusive trends. The maximum pressure recovery and the minimum distortion both occur for the 11000 Newton case. The inlet total pressure recovery is notable here though, with an average value of 86.1% between all three cases. For a typical free stream podded propulsor a pressure recovery of closer to 98% would be expected. If such relatively lower total pressure air was to be ingested by turbomachinery, it would have an extremely deleterius effect on the overall thermal efficiency of the cycyle. STARC-ABL is still affected by the total pressure loss via a relatively lower NPR for the same FPR, but since there is no engine core the hit to overall thermodynamic efficiency does not manifest itself.

Table 2 Performance data for optimized BLI propulsor designs for a range of different F_{net} values.

$F_{\text{net}}(N)$	FPR	$p_t/p_{t\infty}$	BLI shaft power (kW)	distortion metric
9000	1.30	0.845	2437	0.030
11000	1.32	0.872	2081	0.027
13000	1.32	0.867	1725	0.037

Figure 7 shows the side and front views of the baseline and optimized geometries for the three F^*_{net} cases. The color contours show the total pressure levels around the aircraft, with the front view contours in particular highlighting the distortion in the inlet for the BLI propulsors. In all three optimized cases, we can see a more severe nozzle contraction being used to improve the overall thrust. In addition some shaping on the nozzle plug also helps to alleviate some minor flow separation and give slightly better overall performance. Compared to the baseline geometry, the nacelle walls are a bit thicker near the leading edge and much thinner near the trailing edge compared to the baseline. The pressure contours also indicate that the flow is a bit more uniform exiting the nozzle in the optimized cases.

All cases (baseline and three optimized geometries) have a zone of higher total pressure at the bottom of the BLI propulsor inlet. This would create a one-per-revolution excitation in the fan blades and could potentially require some careful aerostructural design. In future work distortion will be uses as an actual constraint on the optimization, and the geometric freedom of the model will be used to try and alleviate that distortion and make the flow more uniform circumferentially.

V. Conclusions

This paper presents the aeropropulsive design optimization of a BLI propulsor for NASA's STARC-ABL aircraft, using a RANS CFD aerodynamics model coupled to a 1 dimensional thermodynamic cycle model for the BLI fan. The coupled model was constructed using the OpenMDAO framework, which enabled the use of analytic derivatives for efficient gradient based optimization.

The optimization sought to minimize the BLI propulsor shaft power required at a cruise condition of Mach .785 and 37000 ft. The aerodynamic model included the fuselage, tail, BLI propulsor, and the wing. A distortion metric based on the ARP-1420 inlet standard was included as a computed quantity, but not directly constrained as part of the optimization. The propulsion model included a variation in fan efficiency as a function of fan pressure ratio. The aeropropulsive coupling was accomplished via a new flow averaging scheme that conserves force and energy flow across the interface plane between the aerodynamics and propulsion.

Three optimizations were run for different values of the constraint on the net force over the whole body, F_{net}, representing three different sized propulsors. The optimized results all found the lowest FPR allowed by the constraints

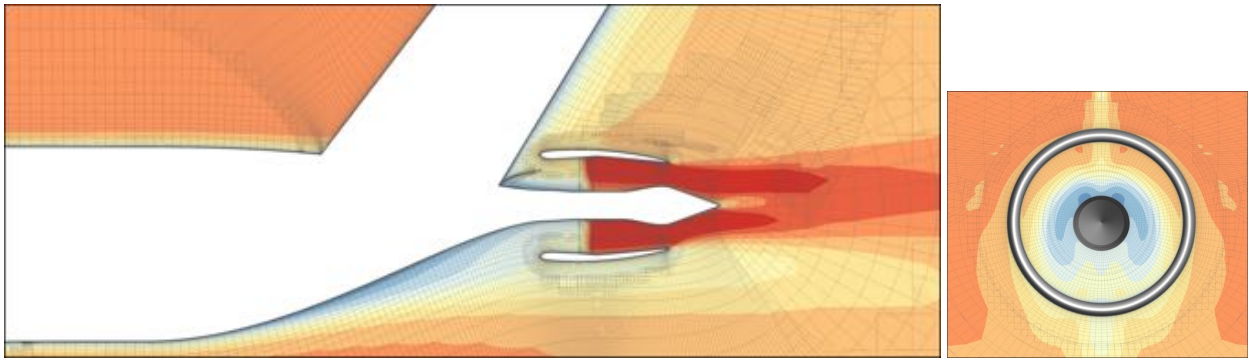

(a) Baseline Geometry

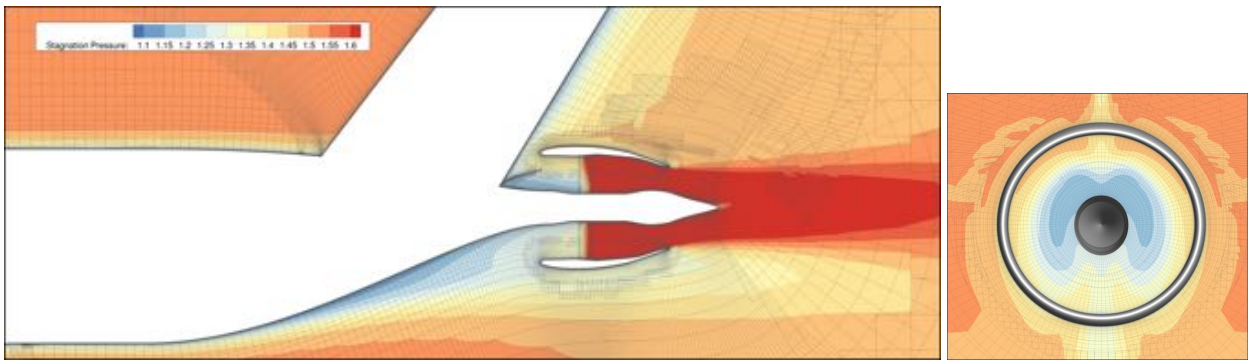

(b) $F^*_{\mathbf{net}}$ = 9000 N

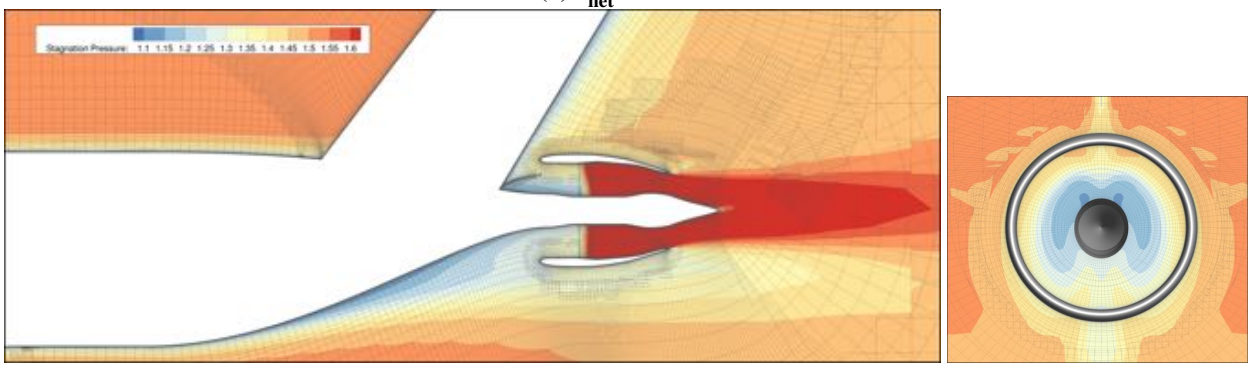

(c) $F^*_{\mathbf{net}}$ = 11000 N

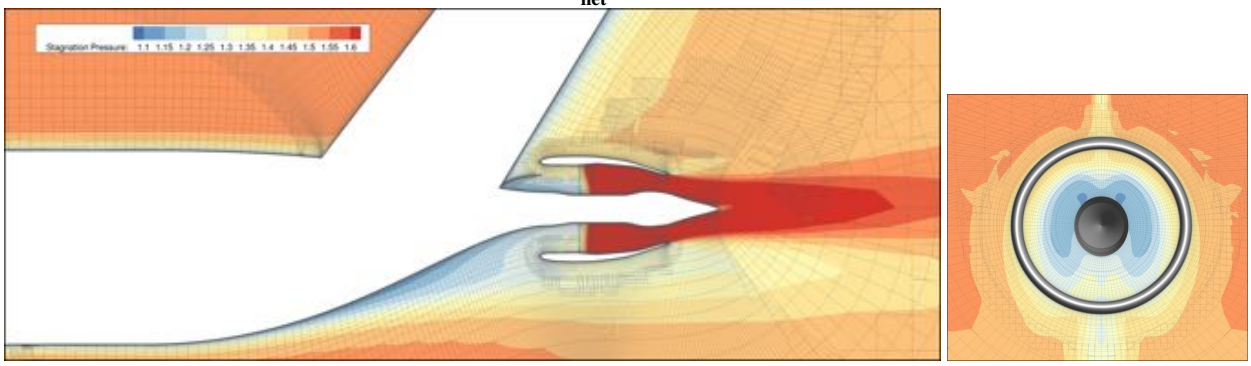

(d) $F^*_{\mathbf{net}}$ = 13000 N

Fig. 7 Contours of stagnation pressure for the baseline and three optimized geometries.

on the problem, choosing to vary the nacelle diameter to accomplish the change in required force from the propulsor. All results showed a noticeable distortion pattern due to the 3 dimensional aerodynamics, including affects from the vertical tail and the wing down wash. Future work will add a constraints on distortion metric to the optimization problem in order to leverage the shape optimization to mitigate some of the distortion effects.

This work represents a preliminary step toward aeropropulsive design optimization of a full aircraft propulsion system. The next step is to integrate a full under wing propulsor model and run optimizations of the full aircraft configuration.

References

[1] Smith, A. M. O., and Roberts, H. E., "The Jet Airplane Utilizing Boundary Layer Ingestion for Propulsion," *Journal of Aeronautical Sciences*, Vol. 14, No. 2, 1947, pp. 97–109.

[2] Wislicenus, G. F., "Hydrodynamics and Propulsion of Submerged Bodies," *Journal of the American Rocket Society*, Vol. 30, 1960, pp. 1140–1148.

[3] Betz, A., *Introduction to the Theory of Flow Machines*, Pergamon Press, 1966.

[4] Gearhart, W. S., and Henderson, R. E., "Selection of a Propulsor for a Submersible System," *Journal of Aircraft*, Vol. 3, No. 1, 1966, pp. 84–90.

[5] Smith, L. H., "Wake Ingestion Propulsion Benefit," *Journal of Propulsion and Power*, Vol. 9, No. 1, 1993, pp. 74–82. doi:10.2514/6.1991-2007.

[6] Drela, M., "Power Balance in Aerodynamic Flows," *AIAA Journal*, Vol. 47, No. 7, 2009, pp. 1761–1771. doi:10.2514/1.42409.

[7] Daggett, D. L., Kawai, R., and Friedman, D., *Blended Wing Body Systems Studies: Boundary Layer Ingestion Inlets With Active Flow Control*, 2003. NASA CR-2003-212670.

[8] Felder, J. L., Kim, H. D., and Brown, G. V., "Turboelectric Distributed Propulsion Engine Cycle Analysis for Hybrid-Wing-Body Aircraft," *47th AIAA Aerospace Sciences Meeting including The New Horizons Forum and Aerospace Exposition*, 2009. doi:10.2514/6.2009-1132, aIAA 2009-1132.

[9] Drela, M., "Development of the D8 Transport Configuration," *9th AIAA Applied Aerodynamics Conference*, 2011. doi:10.2514/6.2011-3970, aIAA 2011-3970.

[10] Liu, C., Doulgeris, G., Laskaridis, P., and Singh, R., "Thermal cycle analysis of turboelectric distributed propulsion system with boundary layer ingestion," *Aerospace Science and Technology*, Vol. 27, No. 1, 2013, pp. 163 – 170. doi:http://dx.doi.org/10.1016/j.ast.2012.08.003.

[11] Laskaridis, P., Pachidis, V., and Pilidis, P., "Opportunities and challenges for distributed propulsion and boundary layer ingestion," *Aircraft Engineering and Aerospace Technology*, Vol. 86, No. 6, 2014, pp. 451–458. doi:10.1108/AEAT-05-2014-0067.

[12] Welstead, J. R., and Felder, J. L., "Conceptual Design of a Single-Aisle Turboelectric Commercial Transport with Fuselage Boundary Layer Ingestion," *54th AIAA Aerospace Sciences Meeting*, 2016. doi:10.2514/6.2016-1027, aIAA 2016-1027.

[13] Gray, J. S., Mader, C. A., Kenway, G. K. W., and Martins, J. R. R. A., "Modeling Boundary Layer Ingestion Using a Coupled Aeropropulsive Analysis," *AIAA Journal of Aircraft*, 2017. doi:10.2514/1.C034601.

[14] "Aerodynamic shape optimization of the STARC-ABL concept for minimal inlet distortion," , January 2018. doi:10.2514/6.2018-1912.

[15] Gill, P. E., Murray, W., and Saunders, M. A., "SNOPT: An SQP Algorithm for Large-Scale Constrained Optimization," *SIAM Rev.*, Vol. 47, No. 1, 2005, pp. 99–131. doi:10.1137/S0036144504446096, URL `http://dx.doi.org/10.1137/S0036144504446096`.

[16] Gray, J. S., Hearn, T. A., Moore, K. T., Hwang, J. T., Martins, J. R. R. A., and Ning, A., "Automatic Evaluation of Multidisciplinary Derivatives Using a Graph-Based Problem Formulation in OpenMDAO," *15th AIAA/ISSMO Multidisciplinary Analysis and Optimization Conference*, American Institute of Aeronautics and Astronautics, 2014. doi:10.2514/6.2014-2042.

[17] Kenway, G. K. W., Secco, N. R., Martins, J. R. R. A., Mishra, A., and Duraisamy, K., "An Efficient Parallel Overset Method for Aerodynamic Shape Optimization," *Proceedings of the 58th AIAA/ASCE/AHS/ASC Structures, Structural Dynamics, and Materials Conference, AIAA SciTech Formum*, 2017. doi:10.2514/6.2017-0357.

[18] Secco, N. R., Jasa, J. P., Kenway, G. K. W., and Martins, J. R. R. A., "Component-based Geometry Manipulation for Aerodynamic Shape Optimization with Overset Meshes," *18th AIAA/ISSMO Multidisciplinary Analysis and Optimization Conference*, 2017.

[19] Hahn, A., "Vehicle Sketch Pad: a Parametric Geometry Modeler for Conceptual Aircraft Design," *48th AIAA Aerospace Sciences Meeting Including the New Horizons Forum and Aerospace Exposition, Aerospace Sciences Meetings*, 2010. AIAA 2010-657.

[20] Luke, E., Collins, E., and Blades, E., "A fast mesh deformation method using explicit interpolation," *Journal of Computational Physics*, Vol. 231, No. 2, 2012, pp. 586 – 601. doi:10.1016/j.jcp.2011.09.021.

[21] Hall, D. K., Greitzer, E. M., and Tan, C. S., "Analysis of Fan Stage Design Attributes for Boundary Layer Ingestion," *ASME. Turbo Expo: Power for Land, Sea, and Aif; Volume 2A: Turbomachinery*, 2016. doi:10.1115/GT2016-57808.

[22] Gray, J., Chin, J., Hearn, T., Hendricks, E., Lavelle, T., and Martins, J. R. R. A., "Chemical Equilibrium Analysis with Adjoint Derivatives for Propulsion Cycle Analysis," *Journal of Propulsion and Power*, Vol. 33, No. 5, 2017, pp. 1041–1052. doi:10.2514/1.B36215.

[23] Hearn, D. T., Hendricks, E., Chin, J., Gray, J., and Moore, D. K. T., "Optimization of Turbine Engine Cycle Analysis with Analytic Derivatives," *17th AIAA/ISSMO Multidisciplinary Analysis and Optimization Conference, part of AIAA Aviation 2016 (Washington, DC)*, 2016. doi:10.2514/6.2016-4297.

[24] Jones, S., *An Introduction to Thermodynamic Performance Analysis of Aircraft Gas Turbine Engine Cycles Using the Numerical Propulsion System Simulation Code*, 2007. NASA TM-2007-214690.

[25] Livesey, J. L., and Hugh, T., "'Suitable Mean Values' in One-Dimensional Gas Dynamics," *Journal of Mechanical Engineering Science*, Vol. 8, No. 4, 1966, pp. 374–383. doi:10.1243/JMES_JOUR_1966_008_049_02.

[26] Livesey, J. L. (ed.), *Flow property averaging methods for compressible internal flows*, 1982. doi:10.2514/6.1982-135.

[27] Jones, S. M., Haller, W. J., and Tong, M. T., *An N+3 Technology Level Reference Propulsion System*, 2017. NASA/TM—2017-219501.

[28] Lambe, A. B., and Martins, J. R. R. A., "Extensions to the Design Structure Matrix for the Description of Multidisciplinary Design, Analysis, and Optimization Processes," *Structural and Multidisciplinary Optimization*, Vol. 46, 2012, pp. 273–284. doi:10.1007/s00158-012-0763-y.

[29] International, S., *Gas turbine inlet flow distortion guidelines. Aerospace Recommended Practice ARP1420*, 2017.

[30] Kreisselmeier, G., and Steinhauser, R., "Systematic Control Design by Optimizing a Vector Performance Index," *International Federation of Active Controls Symposium on Computer-Aided Design of Control Systems, Zurich, Switzerland*, 1979.